Modelling and Optimization of Sandwich Panels for Noise Reduction

Francisco João de Sousa Vieira
francisco.sousa.vieira@tecnico.ulisboa.pt

Instituto Superior Técnico, Universidade de Lisboa, Portugal

June 2019

Abstract

Structures in the transportation industry should be optimized for cost, weight, vibration and noise attenuation, which are important competitiveness issues nowadays. In this framework, sandwich composite panels may represent an optimized solution for both sound radiation and structural vibration for most frequency ranges. The present work addresses vibration and noise reduction in laminated sandwich plates using both viscoelastic and piezoelectric elements, using the capabilities of the commercial software programme ANSYS. The work starts by presenting a state of the art regarding the topics of interest of this work. The sound radiation characteristics of different panels are tested by computing their radiated sound power, using the Rayleigh integral method. Improvements to the panels are made throughout the work by using composite structures, such as electro-viscoelastic sandwich. In the low frequency range, noise and vibration damping can be accomplished through piezoelectric patches bonded to the surfaces of the sandwich panels. For higher frequency ranges, damping is obtained from viscoelastic materials that are used as the core of the sandwich panels. Optimization of thicknesses, fibre orientation of the composite layers and location of the piezoelectric patches is also conducted for minimization of weight and radiated sound power with the use of both Matlab and ANSYS. Results are presented to illustrate the performance of the optimized sandwich panels in terms of weight and noise reduction efficiency.
Keywords: Sandwich structures, Piezoelectricity, Viscoelasticity, Passive Damping, Optimization

1. Introduction

In the transportation industry, noise cancellation is an important competitive issue, since its reduction can lead to better costumer comfort. In that regard sandwich composite panels may represent an optimized solution for both sound radiation and structural vibration in most frequency ranges. Several works devoted to the numerical study of vibration and noise reduction can be found in the literature. Particularly, works in which the aim is to study the characteristics of sandwich panels with viscoelastic and piezoelectric materials for either passive or active control of structure dynamics. Efficient numerical schemes to solve this kind of problems as well as the application of optimization algorithms to find optimal configurations have been widely researched throughout the last 30 years.

Since the seminal work by Allik and Hughes [1], where both variational formulation and finite element implementation of piezoelectric material were performed, there has been a large amount of research regarding the use of these materials. For instance, active damping, where there both a sensor and an actuator are set to damp the structure on the most efficient way through a controller input; and passive damping, where a circuit is tuned to react accordingly with the structure dynamics. A typical example of research concerning passive damping with piezoelectric materials consists of the shunted damping circuits. Hagood and Flotow [2] proposed the resistive and resonant shunting circuits, which allow to attenuate one target frequency. Since then, several other works have been done using the same type of damping. Good examples of these are the several research works performed by Larbi et al. [3, 4, 5], with particular incidence on noise reduction applications.

As far as active damping is concerned, Araújo et al. ([6, 7]) presented a finite element model formulated to better fit these types of problems. In these works, a negative velocity feedback control law is implemented. Nevertheless, other control laws can also be implemented (as can be found in the literature), presenting different advantages and characteristics. For instance, a comparison between a PID (proportional, integral and derivative)

and LQR (linear quadratic reguralor) control laws is presented in [8]. Active vibration control with ANSYS is covered in [9] with the use of a PID control law. However, when using commercial softwares to implement control laws, some limitations are present. For instance, to implement more sophisticated control laws, a better insight over the system matrices is desirable. Considering that purpose, some exterior software tools have been developed throughout the years. An example of this is the the MOR (Model Order Reduction) developed by Rudnyi and Korvink [10] which allows the extraction of model FEM matrices with reduced order which is more suitable to be worked on control system analysis. More recently, Iurlova et al. [11] developed an algorithm that solved directly the natural frequency problem of electro-viscoelastic structures with electric circuit through the extraction of global FEM matrices from ANSYS. Nevertheless, sometimes it is necessary to develop user codes that can overcome these limitations [7]. These codes have the advantage of being completely user-controlled, and their features can be adjusted to fit the user's needs.

Multi-objective optimization has also been linked to the design of sandwich structures over the past few years. Usually the objectives are minimizing the mass, the number of patches, maximizing modal loss factors or even cost minimization. Use of active control, with negative velocity feedback, has been addressed in several occasions, in particular by Araújo et al. [12] and Luis et al.[13]. Madeira et al. also worked in the problem of vibration reduction in [14], to find the set of optimums of constrained layer damping (CLD) patches distributions. The same authors have also published work in multi-objective optimization of a sandwich structures, with thicknesses, stacking sequences and materials as design variables and damping, cost and weight as objective functions [15].

In the present work a study on the active and passive damping of vibrations is made. Then, thicknesses, fibre orientation of the composite layers and location of the piezoelectric patches are optimized in an electro-viscoelastic sandwich panel with the objective of noise reduction. Commercial software ANSYS is used together with Matlab to achieve this purpose.

2. Background

2.1. Orthotropic elastic material

Each lamina of the composite laminated faces of the sandwich plate can be modelled as an orthotropic elastic material. The constitutive equation of an orthotropic material, in its principal material directions is

$$\begin{Bmatrix} \varepsilon_1 \\ \varepsilon_2 \\ \varepsilon_3 \\ \varepsilon_{23} \\ \varepsilon_{13} \\ \varepsilon_{12} \end{Bmatrix} = \begin{bmatrix} s_{11} & s_{12} & s_{13} & 0 & 0 & 0 \\ s_{12} & s_{11} & s_{13} & 0 & 0 & 0 \\ s_{13} & s_{13} & s_{33} & 0 & 0 & 0 \\ 0 & 0 & 0 & s_{44} & 0 & 0 \\ 0 & 0 & 0 & 0 & s_{44} & 0 \\ 0 & 0 & 0 & 0 & 0 & s_{66} \end{bmatrix} \begin{Bmatrix} \sigma_1 \\ \sigma_2 \\ \sigma_3 \\ \sigma_{23} \\ \sigma_{13} \\ \sigma_{12} \end{Bmatrix} =$$

$$\begin{bmatrix} \frac{1}{E_1} & -\frac{\nu_{12}}{E_1} & -\frac{\nu_{13}}{E_1} & 0 & 0 & 0 \\ -\frac{\nu_{12}}{E_1} & \frac{1}{E_2} & -\frac{\nu_{32}}{E_3} & 0 & 0 & 0 \\ -\frac{\nu_{13}}{E_1} & -\frac{\nu_{32}}{E_3} & \frac{1}{E_3} & 0 & 0 & 0 \\ 0 & 0 & 0 & \frac{1}{G_{23}} & 0 & 0 \\ 0 & 0 & 0 & 0 & \frac{1}{G_{13}} & 0 \\ 0 & 0 & 0 & 0 & 0 & \frac{1}{G_{12}} \end{bmatrix} \begin{Bmatrix} \sigma_1 \\ \sigma_2 \\ \sigma_3 \\ \sigma_{23} \\ \sigma_{13} \\ \sigma_{12} \end{Bmatrix} \tag{1}$$

where ε_{ij} are the elastic strain components, σ_{ij} are the corresponding stress components in the principal material directions and s_{ij} are the components of the compliance matrix, also represented in terms of the usual engineering moduli E_i, G_{ij} and ν_{ij}.

2.2. Viscoelastic material

Using the elastic-viscoelastic equivalence principle, a problem with viscoelastic materials in the frequency domain can be solved as an elasticity problem [16], where the complex moduli are given by

$$E_i(j\omega) = E_i^{'}(\omega)\left(1 + j\eta_{E_i}(\omega)\right) \tag{2a}$$

$$G_{ij}(j\omega) = G_{ij}^{'}(\omega)\left(1 + j\eta_{G_{ij}}(\omega)\right) \tag{2b}$$

$$\nu_{ij}(j\omega) = \nu_{ij}^{'}(\omega)\left(1 + j\eta_{\nu_{ij}}(\omega)\right) \tag{2c}$$

and where primed (') quantities denote storage moduli and η denotes the material loss factor. The product between the storage modulus and the loss factor is the loss modulus.

2.2.1. Fractional derivative models

Classical viscoelastic models deal only with spring and dashpot elements, meaning integer order time derivatives are involved, while fractional derivative models are a more powerful way to describe viscoelastic behaviour since they allow the use of non-integer derivatives. Therefore, more accurate behaviour of viscoelastic materials can be captured with the use of these models.
A model that describe well the overall behaviour of a viscoelastic material is the five parameter fractional model developed by Pritz [17]. According to this model, the frequency dependent shear modulus for a viscoelastic isotropic material becomes

$$G(j\omega) = G_0 + G_0(d-1)\frac{(j\omega\tau)^{\alpha}}{1 + (j\omega\tau)^{\beta}} \tag{3}$$

where $d = \frac{G_\infty}{G_0}$ is the ratio of high-frequency limit value of the dynamic shear modulus, G_∞, to the

static shear modulus, G_0, the order of the derivatives of strain and stress are α and β, respectively, and τ is the relaxation time. For more details the reader is referred to reference [17].

2.3. Piezoelectric material

For a transversely isotropic piezoelectric material the constitutive equations are given by

$$\begin{Bmatrix} \sigma_x \\ \sigma_y \\ \sigma_z \\ \sigma_{yz} \\ \sigma_{xz} \\ \sigma_{xy} \end{Bmatrix} = \begin{bmatrix} c_{11} & c_{12} & c_{13} & 0 & 0 & 0 \\ c_{12} & c_{11} & c_{13} & 0 & 0 & 0 \\ c_{13} & c_{13} & c_{33} & 0 & 0 & 0 \\ 0 & 0 & 0 & c_{44} & 0 & 0 \\ 0 & 0 & 0 & 0 & c_{44} & 0 \\ 0 & 0 & 0 & 0 & 0 & c_{66} \end{bmatrix}^E \begin{Bmatrix} \varepsilon_x \\ \varepsilon_y \\ \varepsilon_z \\ \varepsilon_{yz} \\ \varepsilon_{xz} \\ \varepsilon_{xy} \end{Bmatrix} - \begin{bmatrix} 0 & 0 & 0 & 0 & e_{15} & 0 \\ 0 & 0 & 0 & e_{15} & 0 & 0 \\ e_{31} & e_{31} & e_{33} & 0 & 0 & 0 \end{bmatrix}^T \begin{Bmatrix} E_1 \\ E_2 \\ E_3 \end{Bmatrix} \tag{4a}$$

$$\begin{Bmatrix} D_1 \\ D_2 \\ D_3 \end{Bmatrix} = \begin{bmatrix} 0 & 0 & 0 & 0 & e_{15} & 0 \\ 0 & 0 & 0 & e_{15} & 0 & 0 \\ e_{31} & e_{31} & e_{33} & 0 & 0 & 0 \end{bmatrix} \begin{Bmatrix} \varepsilon_x \\ \varepsilon_y \\ \varepsilon_z \\ \varepsilon_{yz} \\ \varepsilon_{xz} \\ \varepsilon_{xy} \end{Bmatrix} + \begin{bmatrix} \in_{11} & 0 & 0 \\ 0 & \in_{11} & 0 \\ 0 & 0 & \in_{33} \end{bmatrix}^S \begin{Bmatrix} E_1 \\ E_2 \\ E_3 \end{Bmatrix} \tag{4b}$$

in which σ_{ij} are the components of the stress vector, c_{ij}^E are the components of the elasticity matrix evaluated at constant electric field, e_{ij} are the components of the piezoelectric coefficient matrix (which couples the structural and electric fields), E_i denotes the components of the electric field vector, ε_{ij} are the components of the strain vector, D_i are the components of the electric displacement vector and $\in_{ij}^S$ are the components of the dielectric matrix, evaluated at constant strain.

2.4. Shunted damping

Shunted damping is a type of structural damping that consists of an electrical circuit, with a resistance R and an inductor L, connected to the electrodes of a piezoelectric material. In this work an RL resonant shunt is used, consisting of an RL circuit with the resistance and the inductor in series. This circuit is then connected to the piezoelectric patch, which acts as a capacitor, as depicted in Figure 3. This assembly forms the well known LRC circuit, that one can take advantage of by tuning its resonant electrical frequency to the mechanical resonant frequency of the system. Knowing the system natural frequency of interest ω_n, the inductor value L can be calculated by

$$\omega_n = \frac{1}{L_i C_{pi}^S} \Leftrightarrow L_i = \omega_n^2 C_{pi}^S \tag{5}$$

where C_{pi}^S is the capacitance of the piezoelectric patch. In [2], Hagood et al. derived and expression for the resistance to obtain the optimal system damping:

$$R_i = \frac{\sqrt{2K_{ij}^2}}{C_{pi}^S \omega_n \left(1 + K_{ij}^2\right)} \tag{6}$$

where K_{ij} is the generalized electromechanical coupling coefficient, which can be calculated easily through the short-circuit (SC) and open-circuit (OC) natural frequencies, using the following expression:

$$K_{ij}^2 = \frac{\left(\omega_n^{OC}\right)^2 - \left(\omega_n^{SC}\right)^2}{\left(\omega_n^{SC}\right)^2} \tag{7}$$

2.5. Active control

The concept of active control contrasts with the one of passive control. Unlike passive control, in active control there is external actuation in order to have a better behaviour of the structure.

Its practical implementation is through a piezoelectric patch collocated below the structure, acting as a sensor, and a piezoelectric patch collocated above, acting as an actuator. The PID controller equation, in the frequency domain is given by

$$U(s) = K_p E(s) + K_i \frac{E(s)}{s} + K_d s E(s) \tag{8}$$

in which $U(s)$ is the actuation, $E(s)$ is the signal from the sensor, K_p, K_i, K_d are the controller design parameters and s is the Laplace variable, such that $s = j\omega$. In the context of piezoelectric transducers, $U(s)$ would be the actuation voltage applied and $E(s)$ would be the voltage in the sensor. Changing variables the equation can be written as (assuming harmonic vibrations)

$$\phi_a = \left(\frac{K_i}{j\omega} + K_p + K_d j\omega\right) \phi_s \tag{9}$$

where the subscript ϕ_a is the voltage of the actuator and ϕ_s is the voltage of the sensor.

2.6. Radiated sound power

When subjected to external excitation, the sound power that is radiated through an area S of the sandwich panel in a semi-infinite rigid baffle is given by:

$$\Pi = \frac{1}{2} \Re \left\{ \int_S p(G) v_n^H(G)\, dS \right\} \tag{10}$$

where S is the area of the radiating panel, G is a point on the plate surface, p is the sound pressure in the fluid and v_n^H is the complex conjugate of the normal velocity of the surface of the plate. While the velocity can be obtained almost automatically

from the displacement (nodal solution) of the finite element model, if the fluid is not discretized one can use the Rayleigh integral to calculate the pressure [18]:

$$p(\omega, M) = \rho_0 \frac{i\omega}{2\pi} \int_S v_n(\omega, G) \frac{e^{-ikr}}{r} \, dS \qquad (11)$$

where ρ_0 is the fluid density, k is the wave number given by $\frac{\omega}{c_0}$, c_0 is the sound speed in the fluid domain, M is a point inside the external acoustic domain and $v_n(\omega, G)$ is the normal velocity at point G.

One way to calculate this integral is through the elementary radiators method. Using this technique, the plate is divided into elementary subdomains (as in the finite element method) and the velocities and pressures used in the calculations are the ones in the center of the elements. Equation (10) becomes:

$$\Pi = \frac{S_e}{2} \Re \left\{ \mathbf{v}_n^H \mathbf{p} \right\} \qquad (12)$$

where S_e is the area of each elementary radiator. Expanding the pressure, the last equation becomes

$$\Pi = \mathbf{v}_n^H \mathbf{R} \mathbf{v}_n^H \qquad (13)$$

where the radiation resistance matrix is given by:

$$\mathbf{R} = \frac{\omega^2 \rho_0 S_e^2}{4\pi c_0} \begin{bmatrix} 1 & \frac{sin(kr_{12})}{kr_{12}} & \cdots & \frac{sin(kr_{1R})}{kr_{1R}} \\ \frac{sin(kr_{21})}{kr_{21}} & 1 & \cdots & \frac{sin(kr_{2R})}{kr_{2R}} \\ \vdots & \vdots & \ddots & \vdots \\ \frac{sin(kr_{R1})}{kr_{R1}} & \frac{sin(kr_{R2})}{kr_{R2}} & \cdots & 1 \end{bmatrix} \qquad (14)$$

3. Preliminary Analyses

3.1. Active control

An iterative loop was implemented in Matlab together with ANSYS in order to implement a PID controller. The code starts with guessed values for the real and imaginary components of the sensor voltage, which are given to calculate the actuator voltage through equation (9). The calculated values are given to ANSYS, which calculates the response in one frequency. If the difference between the guessed and obtained sensor voltage value is within some defined tolerance, the code advances to the next frequency. Otherwise, Matlab function `fsolve` is used in order to obtain the value in which the values of sensor voltage converge. This process takes place in each frequency step. The controlled structure is a $0.15 \times 0.38 \times 0.00081$ m aluminium plate with two $0.266 \times 0.09 \times 0.00081$ m piezoelectric patches. The aluminium plate has the following properties: $E = 70$GPa, $\rho = 2700$kg/m^3, $\nu = 0.33$. The piezoelectric properties are the following: $c_{11} = 126$ GPa, $c_{22} = 126$ GPa, $c_{33} = 117$ GPa, $c_{13} = 84.1$ GPa, $c_{23} = 84.1$ GPa, $c_{12} = 79.5$ GPa, $c_{44} = 23$ GPa, $c_{55} = 23$ GPa, $c_{66} = 23.3$ GPa; $e_{15} = 17$ C/m^2, $e_{24} = 17$ C/m^2, $e_{33} = 23.3$ C/m^2, $e_{31} = -6.5$ C/m^2, $e_{32} = -6.5$ C/m^2; $\in_{11} = 150.3 \times 10^{-10}$ F/m, $\in_{22} = 150.3 \times 10^{-10}$ F/m, $\in_{33} = 130 \times 10^{-10}$ F/m; $\rho = 7500$ kg/m^3.

3.1.1. Results

The influence of the PID controller and its parameters is now studied. Figure 1 presents a comparison of the center point displacement of the PID controller with different parameters. By inspection of the plots presented, one can observe that the increase in magnitude of K_d causes a magnitude decrease of the resonances, despite not changing the static rigidity. The influence of K_p is also visible, since its increase in absolute value causes a decrease of static rigidity value. Regarding the influence of K_i, it can be seen that the plots remain almost the same. In the center point displacement plot, at the lower frequencies there is a deviation that increases with the increase of the magnitude of K_i. It is also noticeable a slight increase of the first resonance amplitude.

3.2. Shunted damping

The influence of introducing a shunted damping RL circuit is now studied. Note that in this case only one patch is used, on top of the aluminium plate. In figure 2 the RSP response of the damped structure is compared to the structure with open circuited patch. By inspection of this figure it is visible the effect of the RL circuit in the first natural frequency, lowering the value of the RSP to about 10^{-3}W.

Although the implementation of PID controller was done successfully, the developed scheme is not computationally efficient, since it takes about 5 hours to run the analysis in the whole frequency range. Hence, the work will progress by improving solutions using other types of vibration reduction techniques, namely by using RL shunted damping.

4. Optimized structure implementation

The addressed structure is a sandwich plate. The core is made of a viscoelastic material, and the top and bottom faces are made of carbon fibre composite laminates. Piezoelectric patches are bonded to the top of the plate, and shunted RL circuits can be connected to each patch. This forms the electro-viscoelastic sandwich panel as shown in Figure 3. The material used for the face layers of the sandwich is carbon fibre, with properties: $E_1 = 130.8$ GPa, $E_2 = 10.6$ GPa, $E_3 = 10.6$ GPa, $\nu_{12} = 0.36$, $\nu_{23} = 0.767$, $\nu_{13} = 0.36$, $G_{12} = 5.6$ GPa, $G_{23} = 3.0$ GPa, $G_{13} = 4.2$ GPa and $\rho = 1543$ kg/m^3. Three layers are considered for each face of the sandwich, with symmetric layup.

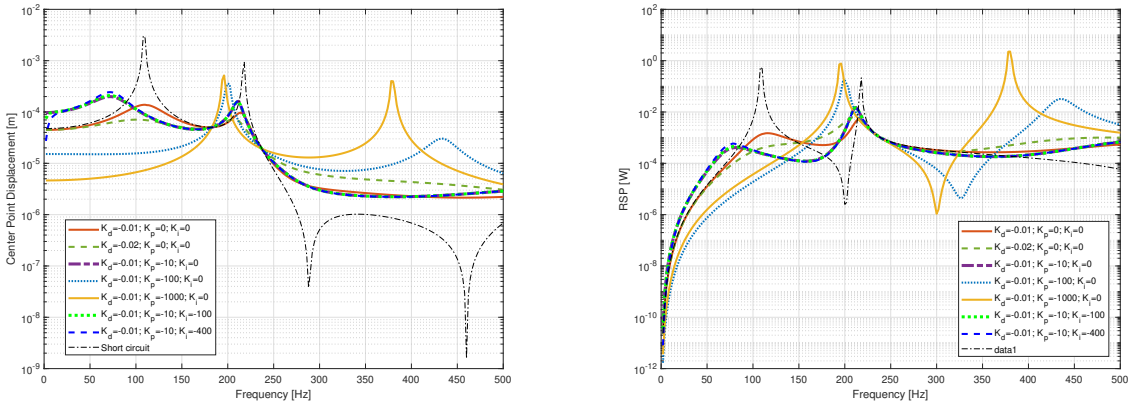

(a) Center point displacement

(b) RSP

Figure 1: Comparison of the performance of the different PID controllers

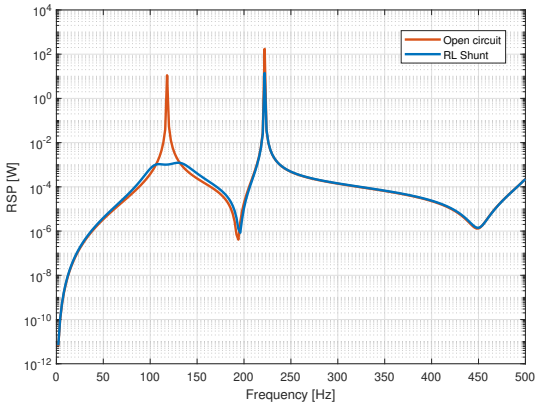

Figure 2: RL Shunt effect

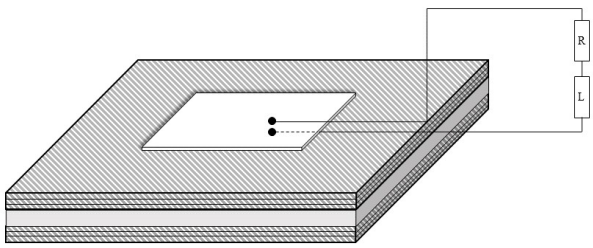

Figure 3: Electro-viscoelastic sandwich panel

The parameters for the viscoelastic core material are: $d = 570$, $\alpha = 0.566$, $\beta = 0.558$, $\tau = 7.23 \times 10^{-10}$, $G_0 = 0.8MPa$, the Poisson's ratio is $\nu = 0.49$ and the mass density is $\rho = 1300$ kg/m^3. Regarding the piezoelectric material, its properties are the same used for the preliminary analyses.

The sandwich has fixed in-plane dimensions of 200×300 mm^2 and is modelled in ANSYS with a solid-shell element, SOLSH190, and the piezoelectric elements are modelled with SOLID5 elements. Both elements have 8 nodes. SOLSH190 has 3 degrees of freedom at each node (3 translations) and SOLID5 has 4 nodal degrees of freedom (3 translations and 1 electric potential). To model the electric circuit elements CIRCU94 is used, which is a line element with 2 nodes and 1 degree of freedom at each node (electric potential). Different element options are used depending on the type of electric component (resistance or inductance).

The sandwich plate structure is simply supported, and has a pressure load of 200 Pa applied to the bottom face.

5. Sandwich panel optimization

With the aim of reducing the levels of acoustic emission of the sandwich structure a first optimization will be conducted. With the objective of reducing the acoustic levels without the addition of any external elements (e.g. without piezoelectric patches), the radiated sound power (RSP) will be minimized in a given frequency range. This will be accomplished by choosing the objective function to minimize as the length of the radiated sound power curve in that frequency range. The design variables in this first optimization will be the thicknesses of the core and laminated carbon fibre layers and also the orientation angles of the layers of the carbon fibre plies.

Mathematically, the optimization problem can be formulated as

$$\begin{aligned} \min_{\mathbf{x}\in\Omega} \quad & f(\mathbf{x}) \\ \text{s.t.} \quad & 1.016\,\text{mm} \leq \mathbf{x}_{CoreThickness} \leq 10.030\,\text{mm}; \\ & 0.17\,\text{mm} \leq \mathbf{x}_{PlyThickness} \leq 1.02\,\text{mm}; \\ & -89^\circ \leq \mathbf{x}_{Angle} \leq 90^\circ; \end{aligned} \tag{15}$$

where f is the length of the RSP curve and the vector $\mathbf{x}$ is the design variables vector. The design vari-

ables include the three angles and three thicknesses corresponding to the three plies of carbon fibre in each face, plus the thickness of the viscoelastic core (see Figure 4). In total, 7 design variables are considered. Note that the number of plies of the carbon fibre is fixed to three and a symmetric stacking sequence is kept.

The constraints are the lower and upper limits of the angles: -89°and +90°respectively; the lower and upper limits of the thicknesses: 0.17 mm and 1.02 mm for the carbon fibre, and 1.016 mm and 10.03 mm for the viscoelastic core.

5.1. Implementation

A Matlab program was developed to control the optimization process through the `patternsearch` function. To use this function, it is necessary to provide the value of the length of the RSP curve, given the values of the design variables. Initial point and constraints are optional. At the end of the optimization, the `patternsearch` function outputs the optimum set of design variables and the respective value of the objective function.

Besides the lower and upper limits that were imposed to these variables, in order to reduce the computational time, the design variable space was transformed from continuous to discrete. Basically, the thickness of the core varies in multiples of 0.127 mm and the thickness of the carbon fibre in multiples of 0.170 mm. In the case of the angles, they are set to take integer values between -89°and 90°.

When using the pattern search algorithm, it is important to assure that all the variables are properly scaled. For instance, it would be inadequate to have the algorithm using angle values in degrees mixed with lengths in millimetres. Hence it was decided that each of the 7 design variables would be scaled to vary between 0 and 1.

To scale the objective function, the length of the RSP curve is multiplied by a large number (in the present work, 10^6). Then a residual number is subtracted, the length of the frequency range multiplied by 10^6. For example, if the range of the curve is from 2 Hz to 500 Hz, the value to be subtracted is 498×10^6.

Due to the different order of magnitudes of the sensitivities of the objective to the design variables, a three step optimization approach is taken. The first step is the optimization of only the angles. After this an optimization of the thicknesses is made, starting from the optimal angle values from the first step. Finally, starting with the optimum of the last optimization step, all 7 variables were considered simultaneously in the last optimization stage. The results and details can be observed in the next section.

Regarding the finite element mesh, a 20×30 in-plane discretization is used with three elements through the thickness, one for each different sandwich component (one for each face and one for the core).

5.2. Results

A summary of the optimization results can be found in Table 1. It can be seen that the design variable vector $\mathbf{x}$ has a different number of entries depending on the optimization. In the last optimization it has 7 entries, with the first three being the angles and the last 4 the thickness multiplication factors, the first three corresponding to the thickness of the carbon fibre plies and the last one to the thickness of the core. Note that the thickness is obtained by multiplying the multiplication factors by 0.170 mm for the carbon fibre and by 0.127 mm for the core. For the initial point the objective function value is $f_{obj} = 1240.535$

The RSP curves resultant from each optimization stage can be found in Figure 5.

Just by looking at the values in the table, one is able to see that the optimization is much more sensitive to changes in values of the thicknesses. The changes in fibre orientation introduced some improvement in the first optimization, but when compared with optimization of the thicknesses, the latter allowed a larger change in the shape of the curve. It is visible that the value of the thickness of the viscoelastic core reached its highest possible value in the first time that the thicknesses are optimized, which was expected due to the fact that this increase in the core thickness promotes the damping capabilities of the sandwich. In Figure 5 it can be seen that the change in the thicknesses had an effect of reducing the resonant frequencies as well as reducing its the amplitudes.

6. Optimization of the piezoelectric material distribution

In this section the performance of the previously optimized sandwich plate with respect to attenuation of acoustic emissions will be further improved by using piezoelectric patches with RL shunt circuits tuned to the first resonant frequency. The problem is formulated as determining the optimal distribution of the piezoelectric patches in order to reduce the length of the RSP curve, with all the RL circuits targeted for the first resonant frequency. This optimization problem is a binary problem in which, using a finite element mesh, each sandwich shell element can have a piezoelectric element above it (1) or not (0), depending on the optimizer output. Figure 6 illustrates this idea.

While adding more piezoelectric material will decrease the radiated sound power response, the mass of the structure will increase. A compromise between mass and acoustic response can be achieved

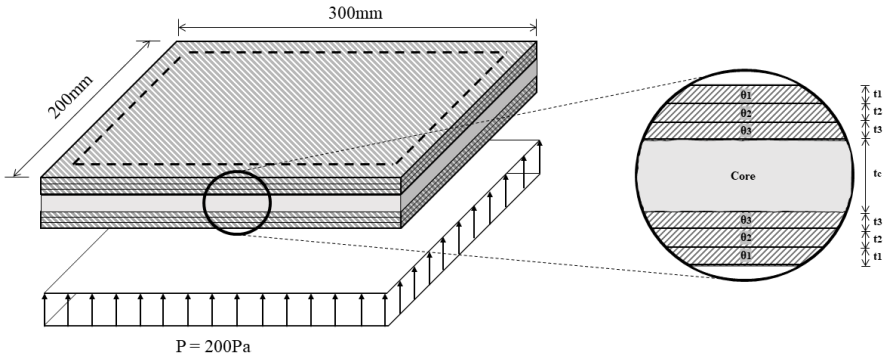

Figure 4: Sandwich structure to be optimized: geometry, boundary conditions and loads.

Table 1: Sandwich optimization results

Optimization	Design Variables	Initial Point	Final Point	f_{obj}
1st Step	$[\theta_1,\theta_2,\theta_3]$	[0°,90°,45°]	[-85°,19°,-1°]	461.213
2nd Step	$[t_1,t_2,t_3,t_c]$	[3,3,3,20]	[2,2,2,79]	10.134
3rd Step	$[\theta_1,\theta_2,\theta_3,t_1,t_2,t_3,t_c]$	[-85°,19°,-1°,2,2,2,79]	[-86°,21°,-1°,2,2,2,79]	10.132

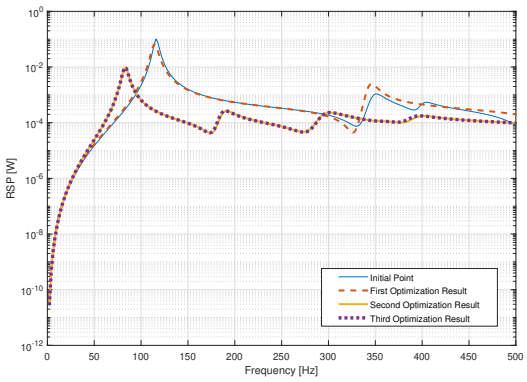

Figure 5: Comparison of the final points of each optimization.

by using multi-objective optimization. The number of piezoelectric regions can also be taken into account and minimized, as each region represents one electroded patch with equipotential conditions imposed on the electrodes, having its own RL circuit. Hence, minimizing the number of regions or patches is the same as minimizing the number of RL circuits. This results in 3 objectives to minimize: the added mass of the piezoelectric patches, the acoustic response and the number of regions. This problem can be formulated as follows:

$$\begin{aligned} \min_{\mathbf{x}\in\Omega} \quad & F(\mathbf{x}) \equiv (f_1(\mathbf{x}); f_2(\mathbf{x}); f_3(\mathbf{x}))^T \\ \text{s.t.} \quad & x_i \in \{0,1\} \end{aligned} \tag{16}$$

in which f_1 is the length of the RSP curve in a given frequency range, f_2 is the total mass of the structure, and f_3 is the number of different piezoelectric patch regions.

6.1. Implementation

Regarding the optimization of the piezoelectric patches, a Matlab program was developed to control the optimization process, in which the function `paretosearch` was used. Similarly to the single-objective optimization described before with the `patternsearch` function, the optimization is controlled by this function, with the user having to supply only the objective function values for each point in the design space and, if needed, initial points and some constraints. The dimension of the design variables vector is the number of elements of piezoelectric finite elements in the model. For instance, if the structure is discretized with a 10×10 mesh, the design variables vector will have dimensions 100×1, in which each entry can take values between 0 and 1 (1 means there is a piezoelectric element and 0 its absence). The majority of the times, the values will not be integer, since the algorithm works with continuous variables. Therefore, if the value is below 0.5 it gets rounded to 0, and otherwise, it is rounded to 1.

Due to the fact that a RL shunt circuit is implemented, the values of the resistance and inductance need to be known *a priori*. Using Equations (5) and (6), the optimal values of the resistance and inductance for a particular resonance can be obtained from the values of ω_n^{OC}, ω_n^{SC} and C_{pi}. Therefore, before conducting the harmonic analysis, two modal analysis have to be done (one with the piezoelectric patches in short-circuit and another in open-circuit) to get the natural frequencies, and a static analysis has to be done in order to get the capacitance. Note that due to the fact that in modal analysis

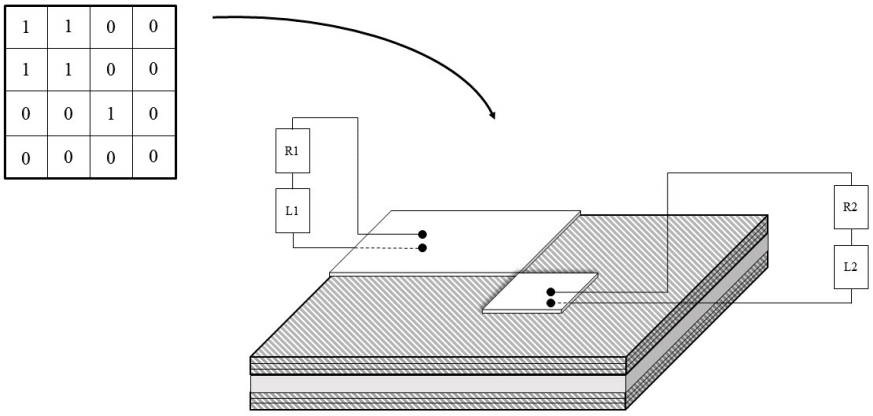

Figure 6: Correspondence between design variables matrix and the sandwich structure

viscoelastic materials are not allowed in ANSYS, a programming loop takes place to get the converged properties of the viscoelastic material at the natural frequency to be obtained.
The added mass is obtained simply by counting the number of piezoelectric elements and then multiplying this number by the volume of each element and the respective density. The calculation of the RSP curve length is conducted as before and the number of regions can be calculated by considering the elements that are adjacent to one another.

Some approaches were used in order to reduce the computational time. For instance, whenever the number of regions was equal or higher than 5, the value of the objective functions were increased several orders of magnitude above the normal values, penalizing these solutions. This avoids running ANSYS to evaluate these points. Another approach to decrease computational time was the reduction of the range of the harmonic analysis: it was decided that only the neighbourhood of the targeted frequency would be analysed: $f_{OC} - 20 < f_{OC} < f_{OC} + 20$ Hz, where f_{OC} is the fundamental resonant frequency in open circuit, in Hz. Also, in this work, a mesh of 6×6 elements was used to generate a first approximation of the solution. The generated solutions were then used as initial points for an optimization using a 12×12 mesh. Then, the resultant points were used as initial points for the final optimization using the most refined 24×24 mesh discretization. This procedure allows the faster convergence of the solutions for larger patch regions. It was also taken advantage of the symmetry of the problem. In fact, by looking at the first mode of vibration of the sandwich, it can be seen that it is symmetric. Hence, the design variables were reduced to $\frac{1}{4}$ of the maximum number of piezoelectric elements.

6.2. Results

As a result of the multi-objective optimization, a set of non-dominated points was obtained, forming the Pareto front. Having 3 objective functions, resulted in a 3D Pareto surface. The evolution of the Pareto front with the different meshes is shown in Figure 7. It is clear that the Pareto front moves to improved solutions with the refinement of the mesh.

A more detailed analysis can be made by choosing 11 distinct Points of the Pareto front, as a better understanding of the behaviour of the structure can be inferred in this way. In Figure 8(a) these points can be observed in the projection of the Pareto front in the plane formed by Objectives 1 and 2. Their RSP curves are displayed in Figure 8(b). These selected points and their design parameters are shown in Table 2. Looking at the results, it can be seen that for less mass the region that starts to be covered by the piezoelectric elements is the centre of the plate which was expected, given the high strain energy in that location for the first mode. It is also important to note that, generally, with more piezoelectric elements a tendency of the frequencies to increase is observed. This is explained by the fact that the stiffness effect introduced dominates the added mass effect. For the configurations with lower mass the R and L values presented are really high. This changes when the added mass increases and the values become more feasible. Even though the first mode was the original target, the other modes get influenced by the added mass. In fact, for configurations 50, 52 and 29, the peak of the second resonant frequencies is almost as high as the magnitude of the first resonant frequency.

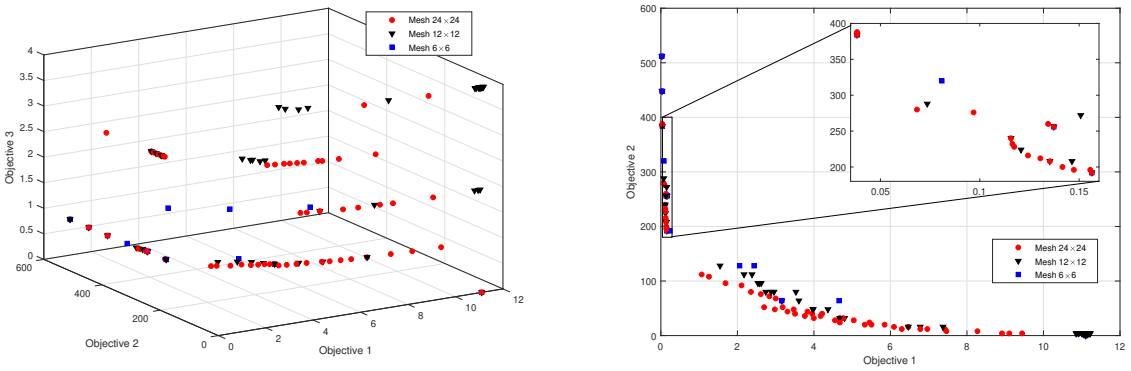

(a) Pareto front

(b) Projection in Objective 1 and 2 plane

Figure 7: Evolution of the Pareto Front with the different meshes. (Objective 1 is the RSP curve length, Objective 2 is the added mass (number of piezoelectric elements) and Objective 3 is the number of regions

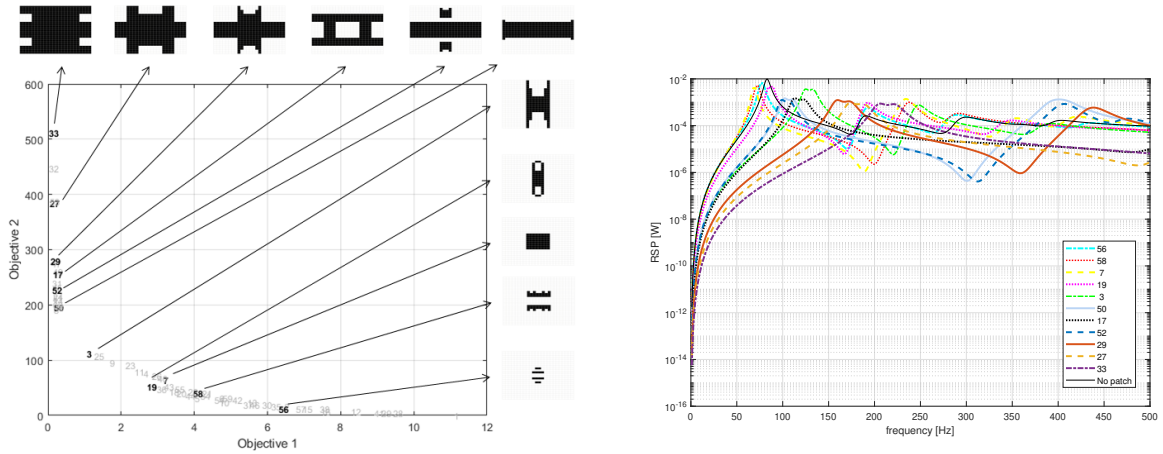

(a) Selected points in the Objective 1 and Objective 2 plane.

(b) RSP vs frequency curves of the selected points

Figure 8: Selected solution points for analysis.

Table 2: Chosen solutions from the multi-objective optimization

#	Mass	No.Regions	R [Ω]	L [H]	f_{SC}[Hz]	f_{OC}[Hz]
56	12	4	36603 18306	3521 1760	77.04	77.05
58	40	2	5827	408	71.92	71.93
7	64	1	1793	139	68.68	68.70
19	52	3	96971 4031	2815 214	86.43	86.51
3	112	1	1987	22.68	128.15	128.53
50	196	1	2027	18.96	105.18	105.86
17	256	1	1426	11.84	116.66	117.43
52	228	3	22535 2125	217.3 20.5	102.2	102.86
29	280	1	838.8	5.44	164.5	165.4
27	384	1	529.38	3.36	178.8	179.67
33	512	1	303.65	1.8	211.9	212.8

7. Conclusions

With the aim of reducing its acoustic response a sandwich structure was optimized with respect to the laminate fibre orientation and ply thicknesses, as well as to its viscoelastic core thickness. To

further reduce the acoustic response, piezoelectric patches with resonant RL shunts were introduced in a multi-objective optimization. The location of the piezoelectric elements were the design variables and the objective functions were the mass, the acoustic response, and the number of shunt circuit regions. The implementation was described and the results were analysed, allowing us to conclude that the proposed methodologies and implementations are efficient and adequate to solve the problem.

References

[1] H. Allik and T. Hughes. Finite element method for piezoelectric vibration, International Journal for Numerical Methods in Engineering. *International Journal for Numerical Methods in Engineering*, 2(2):151–157, 1970.

[2] N. W. Hagood and A. von Flotow. Damping of structural vibrations with piezoelectric materials and passive electrical networks. *Journal ofSound and Vibration*, 142(2):243–268, 1991.

[3] W. Larbi, J. F. Deü, and R. Ohayon. Finite element formulation of smart piezoelectric composite plates coupled with acoustic fluid. *Composite Structures*, 94(2):501–509, 2012.

[4] W. Larbi, J. F. Deü, and R. Ohayon. Finite element reduced order model for noise and vibration reduction of double sandwich panels using shunted piezoelectric patches. *Applied Acoustics*, 108:40–49, 2016.

[5] W. Larbi. Numerical modeling of sound and vibration reduction using viscoelastic materials and shunted piezoelectric patches. *Computers and Structures*, 2017.

[6] A. L. Araújo, C. M.Mota Soares, and C. A.Mota Soares. Finite element model for hybrid active-passive damping analysis of anisotropic laminated sandwich structures. *Journal of Sandwich Structures and Materials*, 12(4):397–419, 2010.

[7] A L Araújo, V S Carvalho, C M Mota Soares, J Belinha, and A J M Ferreira. Vibration analysis of laminated soft core sandwich plates with piezoelectric sensors and actuators. *Composite Structures*, 151:91–98, 2016.

[8] Shunqi Zhang, Rüdiger Schmidt, and Xiansheng Qin. Active vibration control of piezoelectric bonded smart structures using PID algorithm. *Chinese Journal of Aeronautics*, 28(1):305–313, 2015.

[9] H. Karagülle, L. Malgaca, and H. F. Öktem. Analysis of active vibration control in smart structures by ANSYS. *Smart Materials and Structures*, 13(4):661–667, 2004.

[10] E. B. Rudnyi and J. G. Korvink. Model Order Reduction for Large Scale Engineering Models Developed in ANSYS. In *Lecture Notes in Computer Science*, number June 2004, 2004.

[11] Nataliia Iurlova, Natalia Sevodina, Dmitrii Oshmarin, and Maksim Iurlov. Algorithm for solving problems related to the natural vibrations of electro-viscoelastic structures with shunt circuits using ANSYS data. *International Journal of Smart and Nano Materials*, 10(2):156–176, 2019.

[12] A. L. Araújo, J. F A Madeira, C. M. Mota Soares, and C. A. Mota Soares. Optimal design for active damping in sandwich structures using the Direct MultiSearch method. *Composite Structures*, 105:29–34, 2013.

[13] Ndilokelwa F. Luis, J. F.A. Madeira, A. L. Araújo, and A. J.M. Ferreira. Active vibration attenuation in viscoelastic laminated composite panels using multiobjective optimization. *Composites Part B: Engineering*, 128:53–66, 2017.

[14] J. F.A. Madeira, A. L. Araújo, C. M. Mota Soares, and C. A. Mota Soares. Multiobjective optimization for vibration reduction in composite plate structures using constrained layer damping. *Computers and Structures*, 2017.

[15] J. F.A. Madeira, A. L. Araújo, C. M. Mota Soares, C. A. Mota Soares, and A. J.M. Ferreira. Multiobjective design of viscoelastic laminated composite sandwich panels. *Composites Part B: Engineering*, 77:391–401, 2015.

[16] R Christensen. *Theory of Viscoelasticity: An Introduction*. Academic Press, 2nd editio edition, 1982.

[17] T. Pritz. Five-parameter fractional derivative model for polymeric damping materials. *Journal of Sound and Vibration*, 265(5):935–952, 2003.

[18] Frank Fahy and Paolo Gardonio. *Sound and Structural Vibration Radiation, Transmission and Response*. Academic Press, 2nd. editi edition.